Theor Appl Genet (2011) 122:661–675
DOI 10.1007/s00122-010-1476-5

ORIGINAL PAPER

Quantitative trait loci for flowering time and inflorescence architecture in rose

Koji Kawamura · Laurence Hibrand-Saint Oyant · Laurent Crespel · Tatiana Thouroude · David Lalanne · Fabrice Foucher

Received: 10 August 2010 / Accepted: 30 September 2010 / Published online: 3 November 2010

Abstract The pattern of development of the inflorescence is an important characteristic in ornamental plants, where the economic value is in the flower. The genetic determinism of inflorescence architecture is poorly understood, especially in woody perennial plants with long life cycles. Our objective was to study the genetic determinism of this characteristic in rose. The genetic architectures of 10 traits associated with the developmental timing and architecture of the inflorescence, and with flower production were investigated in a F_1 diploid garden rose population, based on intensive measurements of phenological and morphological traits in a field. There were substantial genetic variations in inflorescence development traits, with broad-sense heritabilities ranging from 0.82 to 0.93. Genotypic correlations were significant for most (87%) pairs of traits, suggesting either pleiotropy or tight linkage among loci. However, non-significant and low correlations between some pairs of traits revealed two independent developmental pathways controlling inflorescence architecture: (1) the production of inflorescence nodes increased the number of branches and the production of flowers; (2) internode elongation connected with frequent branching increased the number of branches and the production of flowers. QTL mapping identified six common QTL regions (cQTL) for inflorescence developmental traits. A QTL for flowering time and many inflorescence traits were mapped to the same cQTL. Several candidate genes that are known to control inflorescence developmental traits and gibberellin signaling in *Arabidopsis thaliana* were mapped in rose. Rose orthologues of *FLOWERING LOCUS T* (*RoFT*), *TERMINAL FLOWER 1* (*RoKSN*), *SPINDLY* (*RoSPINDLY*), *DELLA* (*RoDELLA*), and *SLEEPY* (*RoSLEEPY*) co-localized with cQTL for relevant traits. This is the first report on the genetic basis of complex inflorescence developmental traits in rose.

Communicated by H. Nybom.

Electronic supplementary material The online version of this article (doi:10.1007/s00122-010-1476-5) contains supplementary material, which is available to authorized users.

K. Kawamura · L. Hibrand-Saint Oyant · T. Thouroude · D. Lalanne · F. Foucher (✉)
INRA d'Angers Nantes, IFR 149 Quasav, UMR 1259 GenHort, BP60057, 49071 Beaucouzé cedex, France
e-mail: fabrice.foucher@angers.inra.fr

L. Crespel
Meilland International, Domaine Saint André, 83340 Le Cannet des Maures, France

Present Address:
K. Kawamura
Laboratory of Horticultural Science, Graduate School of Bioagricultural Sciences, Nagoya University, Nagoya 464-8601, Japan

Present Address:
L. Crespel
AGROCAMPUS OUEST Centre d'Angers, Institut National d'Horticulture et de Paysage, IFR 149 Quasav, UMR 1259 GenHort, 2, rue Le Nôtre, 49045 Angers Cedex 01, France

Introduction

Roses are economically the most important ornamental, with a wide range of uses as cut flowers, garden and landscaping plants, miniature pot plants and rootstock (Debener and Linde 2009). Roses are also useful for the production of rose oil, for the perfume industry, and for food products (Gudin 2000). Intensive breeding activities, which mainly depend on cross-breeding techniques, have resulted in the creation of

around 30,000 cultivars worldwide. Yet, little is known about the inheritance of important ornamental characteristics in rose, and the success of rose breeding largely depends on chance and empiricism (Gudin 2000). This is because roses are predominantly outcrossing plants and are therefore highly heterozygous. Furthermore, the majority of cultivars are polyploid. Consequently, the inheritance patterns of most characteristics are difficult to predict. In addition, the ease with which roses can be vegetatively propagated does not require the establishment of sophisticated breeding strategies (Debener 1999).

In woody plant species with a long life cycle such as rose, there is major benefit to be had in developing genetic maps to increase our knowledge of the genetic determinism of complex ornamental traits (Debener and Mattiesch 1999). Genetic mapping has enabled the identification of molecular markers potentially useful to assist breeding programs by early seedling selection. Quantitative trait loci (QTL) mapping has been performed in rose in five diploid populations and one tetraploid population (Debener and Linde 2009). The genomic regions controlling the number of petals (Debener and Mattiesch 1999; Crespel et al. 2002; Hibrand-Saint Oyant et al. 2008), blooming date (Dugo et al. 2005; Hibrand-Saint Oyant et al. 2008), prickle density (Crespel et al. 2002; Rajapakse et al. 2001), black spot or powdery mildew resistance (Xu et al. 2005; Linde et al. 2006), flower and leaf size (Dugo et al. 2005), cut rose vigor (Yan et al. 2007), and scent production (Spiller et al. 2010a) have been identified.

The inflorescence is a flower-bearing branching system (Weberling 1992). Inflorescence architecture is a key agronomic characteristic as it largely determines plant productivity (Brown et al. 2006; Upadyayula et al. 2006a, b). The molecular basis of inflorescence development has been extensively studied in model plants and crops, such as *Arabidopsis thaliana* (Bradley et al. 1997), petunia (Souer et al. 1998), rice (Kyozuka et al. 1998), and maize (Bomblies et al. 2003) (see Bhatt 2005; Benlloch et al. 2007 for reviews). However, except for the recent work on grapevine (Marguerit et al. 2009; Fernandez et al. 2010), little work has been performed on woody perennial plants. There are several difficulties involved in the genetic study of inflorescence architecture, especially in woody perennial plants such as rose. First, the huge cost in space and time required to cultivate the plants until the inflorescence architecture becomes apparent. Second, the difficulties involved in quantifying the genetic differences in inflorescence architecture. This is because (1) inflorescence architecture is a complex characteristic with multiple traits (e.g., internode elongation, axillary branching, and the timing of meristem differentiation), (2) variation in inflorescence architecture can be continuous, and (3) some inflorescence traits are likely to change with changes in environmental conditions (i.e., low heritability). Roses have a wide variety of inflorescence architecture ranging from solitary flowers to complex cymes. A simple inflorescence forms one terminal flower and a few lateral flowers, whereas in a compound inflorescence, lateral shoots continuously branch into higher order shoots and produce numerous flowers. Inflorescence architecture is a critical determinant of the value of ornamental roses, especially garden and landscaping roses, as it determines the number of flowers, their arrangement on the plant, and the external appearance of the plant.

The development of the inflorescence in angiosperm plants is based on the spatiotemporal variation of meristem activity (Coen and Nugent 1994). The shoot apical meristem (SAM) generates leaves and shoots during the vegetative phase, and during the reproductive phase after the floral transition, it becomes an inflorescence and flowers are produced. The architecture of the inflorescence depends on when and which meristems give rise to flowers (Coen and Nugent 1994). Prusinkiewicz et al. (2007) proposed a simple developmental model regarding the timing of floral transition of apical and axillary meristems that successfully explains the diverse forms of inflorescence architecture observed in nature. In support of this theory, studies on the genetic basis of inflorescence architecture have demonstrated that the "flowering genes" controlling the initiation of floral meristems largely regulate the architecture of the inflorescence (see Bhatt 2005; Benlloch et al. 2007 for reviews); therefore, flowering genes may be candidate genes for the control of inflorescence architecture.

In rose, *RECURRENT BLOOMING* gene, *RB* was shown to encode a *TERMINAL FLOWER 1* (*TFL1*) homologue, *RoKSN* (unpublished results from our laboratory). Gibberellins (GA) are a key hormone in the control of flowering in rose (Roberts et al. 1999), and GA metabolism and signaling genes may play a critical role in floral initiation (Remay et al. 2009). Homologues of floral integrators in *Arabidopsis*, *FLOWERING LOCUS T* (*FT*) and *SUPPRESSOR OF CONSTANS* (*SOC1*), floral meristem identity genes, *LEAFY* (*LFY*) and *APETALA1* (*AP1*), and organ identity genes, *AGAMOUS* (*AG*) and *PISTILLATA* (*PI*) have been isolated in rose and shown to be induced during floral transition (Kitahara and Matsumoto 2000; Kitahara et al. 2001; Foucher et al. 2008; Remay et al. 2009). These studies provide an opportunity to quickly search for candidate genes for inflorescence development in rose. We therefore aimed (1) to define the genetic variability and the modes of inheritance of inflorescence developmental traits in rose, such as the timing of flowering, number of flowers per shoot, and branching architecture, (2) to determine the genetic architecture i.e., the number and genetic map locations of the loci controlling inflorescence traits, and (3) to test the map

co-localization between some of these flowering genes and the QTL. We identified several putative candidate genes for rose inflorescence development.

Materials and methods

Plant material

A progeny of 98 diploid F_1 hybrids from a cross between diploid roses *TF* × *RW* was used for map construction and QTL analysis. The female parent *TF* is "The Fairy", a commercial cultivar obtained from the cross "*Paul Crampel*" × "*Lady Gay*" in 1932 by Ann Bentall, and the male parent *RW* is a hybrid of *R. wichurana* obtained from Jardin de Bagatelle (Paris, France). *TF* has a pink double-flowered, upright rose with recurrent blooming. *RW* has white flowers with five petals and is a ground-covering rose with single seasonal blooming. Both *TF* and *RW* develop a highly branched, compound inflorescence.

Field cultivation

Plants were grown in a field in Cannet des Maures (Meilland International, France). Three cuttings were collected from each plant and cultivated in a field belonging to INRA, Angers, France, since 2004. Replicate plants were arranged in three rows oppositely arranged in the first and second rows, and randomly planted in the third row. The roses were pruned each winter; three to four vigorous current-year shoots were cut at the 6th node from the base of each plant, and the other shoots were removed. In the following spring, new shoots developed from the axillary buds on the old shoots and were termed "1st order shoots" (Fig. 1); the growth of the 1st order shoot was terminated by the formation of inflorescence. Further growth occurred from "2nd order shoots", which originate from axillary buds on the 1st order shoots. In recurrent blooming roses, all 2nd order shoots again produce inflorescences and the process of flowering and branching continues until the end of autumn (Fig. 1). In contrast, in non-recurrent blooming roses, several 2nd order shoots (especially from the basal part) and most 3rd order shoots remain vegetative and continue to grow during the rest of the growing season.

Phenotypic data collection

The blooming habit (recurrent/non-recurrent blooming) was determined for each plant based on the observation of the presence of flowering shoots during the autumn of 2007 and 2008. The date of flowering (*D1Flower*) was determined as the date when once the petals are visible from under the sepals (*BD*, Hibrand-Saint Oyant et al. 2008) in each of the 4 years from 2006 to 2009.

The 1st order shoot that developed in spring was divided into a vegetative part (*VEG1*) and inflorescence part (*INF1*) based on the changes in leaf morphology from normal leaves (*nL*) to bract-like leaves (*bL*) (Fig. 1). The number

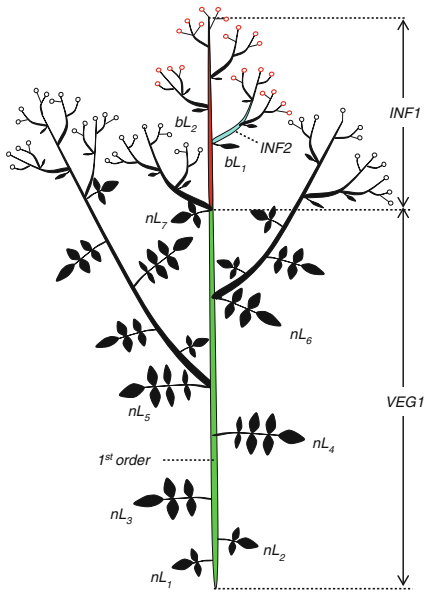

Definition	
nL	Normal leaf with at least 3 leaflets
bL	Bract-like leaf with 1-2 small inmature leaflets
VEG1	Vegetative part of 1st order shoot with *nLs*
INF1	Inflorescence part of 1st order shoot with *bLs*
INF2	The longest 2nd order shoot which develops from *INF1*

Scoring traits	
NV1	Number of nodes on *VEG1*
NF1	Number of nodes on *INF1*
NF2	Number of nodes on *INF2*
LV1	Average length of internodes of *VEG1* (= Length of *VEG1*/ *NV1*)
LF1	Average length of internodes of *INF1* (= Length of *INF1*/ *NF1*)
LF2	Average length of internodes of *INF2* (= Length of *INF2*/ *NF2*)
NBF2	Number of 3rd order shoots on *INF2*
BIF2	% of lateral meristems, which develop into 3rd order shoots (= 100**NBF2*/ *NF2*)
FLW	Total number of flower produced by *INF1*

Fig. 1 Pictorial representation of branching structure of 1st order shoot and inflorescence in recurrent blooming rose. Definitions of terms are on the *right*. *Open circle* indicates a flower. The main axis corresponds to the 1st order shoot, and the lateral shoots developing from the 1st order axis are 2nd order shoots. The boundary between vegetative part (*VEG1*) and the inflorescence (*INF1*) of the 1st order shoot was defined according to the changes in leaf morphology from normal leaves (*nLs*) to bract-like leaves (*bLs*). Trait values of the picture are as follows; *NV1* = 7, *NF1* = 6, *NF2* = 4, *NBF2* = 3, *BIF2* = 75, *FLW* = 22

of nodes and the length of the vegetative and inflorescence parts were determined separately. The number and length of nodes and axillary branches were then measured on the longest 2nd order shoot (*INF2*) of *INF1*. The total number of flowers produced by *INF1* was also counted. Based on these measurements, nine inflorescence traits were obtained (Fig. 1). Measurements were made on an average of 2.7 shoots per plant. We selected 1st order shoots that developed from the underground or basal part of the previous year's stems, because they are generally vigorous and representative of overall plant architecture. Sample selection and measurements were done in each of the 2 years, 2008 and 2009.

Genotypic data collection

Genomic DNA of each genotype of the population was extracted from young unfolded leaves (100 mg) using Dneasy®96 Plant Kit, QIAGEN, following the manufacturer's protocol. A total of 75 molecular markers was used to construct the genetic map. The markers consisted of 57 microsatellite (SSR) markers previously used in rose (Zhang et al. 2006; Hibrand-Saint Oyant et al. 2008; Yan et al. 2005: Spiller et al. 2010a), 12 genes (Kitahara and Matsumoto 2000; Kitahara et al. 2001; Foucher et al. 2008; Remay et al. 2009), and six new genomic markers ("*MarQ*" and "*RoX*-") developed by INRA, France. "*MarQ*" is a SCAR marker developed from AFLP/BSA analysis (Hibrand-Saint Oyant et al. unpublished). The five "*RoX*-" markers were developed either from the rose EST library or by using a degenerate primer strategy and are under investigation by other researchers. Primer sequence information is available on request. Polymerase chain reaction (PCR) amplification was carried out under the conditions described in Hibrand-Saint Oyant et al. (2008) or Remay et al. (2009). The length polymorphism of PCR products was detected by gel electrophoresis or with a capillary sequencer according to the protocol described in Hibrand-Saint Oyant et al. (2008). To map the 12 genes, five *RoX*-markers and some SSRs without clear length polymorphism, sequence polymorphisms of PCR products were analyzed using the single-strand conformation polymorphism (SSCP) method according to the procedure described in Remay et al. (2009).

Phenotypic data analysis

Phenotypic variance of inflorescence traits was partitioned into different components using the following model:

$$P_{ijkl} = u + G_i + Y_j + GY_{ij} + R_{(ij)k} + \varepsilon_{ijkl}$$

where P_{ijkl} is the overall mean phenotypic value of a trait measured on shoot l of plant k in genotype i in year j; u is the overall mean; G_i is the random effect of genotype i; Y_j is the fixed effect of year j; GY_{ij} is the random interaction of genotype i and year j; $R_{(ij)k}$ is the random effect of replicated plant k nested in genotype i and year j; ε_{ijkl} is the random residual error for plant k in genotype i in year j. The phenotypic variance (σ^2_{P}) of a trait can be partitioned into the variance of genotypic effect (σ^2_{G}), genotype × year interaction (σ^2_{GY}), and the variance between replicated plants within the genotype (σ^2_{R}), and residual error variance (σ^2_{E}). The σ^2_{E} includes the variance between replicated shoots within a plant and the error in measurements:

$$\sigma^2_{\mathrm{P}} = \sigma^2_{\mathrm{G}} + \sigma^2_{\mathrm{GY}} + \sigma^2_{\mathrm{R}} + \sigma^2_{\mathrm{E}}$$

Variance components were estimated based on the restricted maximum likelihood (REML) method. The REML method is considered a suitable procedure to estimate variance components for unbalanced data (Dieters et al. 1995). Broad-sense heritability (h^2) based on genotypic mean values averaged across years was calculated as follows (Holland et al. 2003):

$$h^2 = \sigma^2_{\mathrm{G}} / \left(\sigma^2_{\mathrm{G}} + \sigma^2_{\mathrm{GY}}/y + \sigma^2_{\mathrm{R}}/yr + \sigma^2_{\mathrm{E}}/yrs\right)$$

where y is the number of replication years, r is the number of replication plants per genotype, and s is the number of replication shoots per plant. Average numbers of replications per genotype obtained for each trait (Table 1) were used for the calculation. Standard error of heritability was approximated using Dickerson's method (Dieters et al. 1995). Since the flowering time trait (*D1Flower*) was measured at the plant level, the effect of replicated plants was removed from the model, and h^2 was calculated by $h^2 = \sigma^2_{\mathrm{G}}/(\sigma^2_{\mathrm{G}} + \sigma^2_{\mathrm{GY}}/y + \sigma^2_{\mathrm{E}}/yr)$.

Least-square means (LS-means) were computed for each trait for each genotype. The normality of LS-mean distribution of F_1 genotype was examined using the Shapiro–Wilk test. For the traits that significantly differed from the normal distribution ($P < 0.05$), logarithmic or square root transformation was used, and the variance decomposition, heritability estimation, and LS-mean computation were repeated for the transformed values. After transformation, LS-means of all variables were normally distributed (Shapiro–Wilk test, $P > 0.04$). For these traits, the results of transformed values are reported. Genotypic correlations (r_{g}) between traits were estimated using the Pearson product-moment correlation coefficient (Via 1984). LS-means computed for each genotype were used for the estimation of r_{g}. All the phenotypic data analysis was conducted using JMP software version 8.0 (SAS Institute, Inc., Cary, NC, USA).

Genetic map construction

The genetic linkage map was built using JoinMap® 4.0 (Van Ooijen 2006). Log-of-odds (LOD) scores ≥5 were

Table 1 Least-square means (LS-means) and standard error (SE) of parents The Fairy (*TF*) and a hybrid of *R. wichurana* (*RW*), along with ranges of LS-means of F_1 hybrids (range of F_1), estimates of broad-sense heritability at the genotypic mean level (h^2) and percentages of different variance components in total phenotypic variance (σ^2_P), for flowering time and nine inflorescence traits

Trait[c]	Unit	Trs[a]	*TF*		*RW*		Range of F_1	H^2	SE	Percentage (SE) of variance component[b] in σ^2_P							
			LS-mean	SE	LS-mean	SE				σ^2_G	SE	σ^2_{GY}	SE	σ^2_R	SE	σ^2_E	SE
D1Flower	Day	NT	17.51	1.70	13.60	1.70	6.94–31.75	0.92	0.14	**57.1**	8.9	8.8	1.9	NE		34.0	1.8
Log (NV1)	No.	Log_{10}	1.17	0.03	1.09	0.03	0.93–1.46	0.93	0.15	**62.7**	9.8	NS		15.2	1.9	21.4	1.0
NF1	No.	NT	14.47	0.74	11.48	0.74	6.29–19.57	0.92	0.15	**52.6**	8.3	NS		15.0	2.2	32.7	1.5
NF2	No.	NT	6.84	0.45	6.07	0.45	3.91–10.96	0.91	0.15	**48.0**	7.8	NS		13.7	2.3	38.9	1.8
LV1	cm	NT	2.26	0.15	2.37	0.15	1.41–2.89	0.82	0.15	32.6	6.0	NS		31.2	3.6	**38.4**	1.8
LF1	cm	NT	1.51	0.08	1.45	0.08	0.71–1.77	0.89	0.15	**53.3**	9.0	NS		21.0	2.4	23.3	1.1
LF2	cm	NT	1.16	0.09	1.48	0.09	0.52–1.68	0.88	0.15	**50.6**	8.4	NS		21.0	2.5	26.5	1.2
NBF2	No.	NT	5.10	0.56	4.72	0.56	1.26–7.26	0.85	0.15	39.2	7.1	NS		18.8	2.8	**40.1**	1.8
Log (100 − BIF2)	%	Log_{10}	1.35	0.06	1.33	0.06	1.13–1.86	0.86	0.15	37.5	6.5	NS		14.4	2.6	**47.7**	2.2
Sqrt (FLW)	No.	Sqrt	6.64	0.36	6.98	0.36	3.38–9.50	0.93	0.15	**60.2**	9.7	NS		16.0	2.0	23.3	1.1

[a] Transformation of value (*NT* no transformation, *Log_{10}* log-transformed, *Sqrt* square-root-transformed)

[b] Variance components of genotype (σ^2_G), genotype × year interaction (σ^2_{GY}), replicated plants nested into genotype and year (σ^2_R), and residual error (σ^2_E). The largest variance components in each trait are in bold. *NE* not estimated, *NS* not significant ($P > 0.05$)

[c] Average number of repetition of measurements were 2.8 plants per genotype × 4 years (2006–2009) for *D1Flower* (date when once the petals are visible from under the sepals) and 2.7 plants per genotype × 2.7 shoots per plant × 2 years (2008, 2009) for 9 inflorescence traits, including *NV1* (number of nodes on *VEG1*, vegetative part of 1st order shoot), *NF1* (number of nodes on *INF1*, inflorescence part of 1st order shoot), *NF2* (number of nodes on *INF2*, the longest 2nd order shoot of the inflorescence), *LV1* (average internode length of *VEG1*), *LF1* (average internode length of *INF1*), *LF2* (average internode length of *INF2*), *NBF2* (number of 3rd order shoots of *INF2*), *BIF2* (percentage of lateral meristems on *INF2* that develop into 3rd order shoots), *FLW* (total number of flowers produced by *INF1*)

used to determine linkage groups. The order of the markers was determined based on regression mapping by using the pairwise data of only those loci that showed a recombination frequency smaller than 0.45 and a LOD >1. The ripple value of 1 and the jump threshold of 5 were used. According to the pseudo-test cross-strategy (Grattapaglia and Sederoff 1994), parental maps were built separately using uni-parental and common bi-parental markers. The homologous parental linkage groups with common bi-parental markers were then combined, and integrated maps were built based on mean recombination frequencies and combined LOD scores using the 'combine groups for map integration function' in JoinMap® 4.0 (Van Ooijen 2006). Marker segregation distortion was tested against the expected Mendelian segregation ratios using the chi-square test in the software. Maps were drawn using MapChart version 2.1 software (Voorrips 2002).

QTL analysis

QTL analyses were carried out using MAPQTL® 5.0 (Van Ooijen 2004), on the LS-means per genotype and integrated map. Firstly, a LOD threshold at which a QTL was declared significant was determined according to a genome-wide error rate of 0.05 over 1,000 permutations of the data (Churchill and Doerge 1994). Secondly, interval mapping analysis was performed with a step size of 1 cM to find regions with potential QTL effects, i.e., where the LOD score was greater than the threshold. In the region of the potential QTLs, the markers with the highest LOD values were taken as cofactors. A backward elimination procedure was used to select cofactors significantly associated with each trait at $P < 0.02$. Subsequently, multiple QTL mapping (MQM, Jansen and Stam 1994) was performed with a step size of 1 cM. If LOD scores in the region of the potential QTLs were below the significance threshold, their cofactor loci were removed, and MQM mapping was repeated. QTL positions were assigned to local LOD score maxima. Confidence intervals of the map position were indicated in centimorgans corresponding to a 1- or 2-LOD interval. The percentage of σ^2_P explained by each QTL (r^2) was taken from the MQM mapping output %Expl. The total percentage of σ^2_P explained by all significant QTLs in a given trait (R^2) was also calculated. The R^2 was then divided by h^2 (% scale) to estimate the proportion of σ^2_G explained by the QTL. When QTLs for different traits had overlapping confidence intervals, they were declared to be a potentially "common QTL (cQTL)".

Following the method proposed by Knott et al. (1997), allelic effects were estimated as:

$$A_f = (u_{ac} - u_{bc}) + (u_{ad} - u_{bd})/(2SD)$$

$$A_m = (u_{ac} - u_{ad}) + (u_{bc} - u_{bd})/(2SD)$$

$$D = (u_{ac} + u_{bd}) - (u_{ad} + u_{bc})/(2SD)$$

where u_{ac}, u_{bc}, u_{ad}, and u_{bd} are estimated phenotypic means associated with each of the four possible genotypic classes, ac, bc, ad, and bd, deriving from the cross ab (female) × cd (male), and were taken from the MQM mapping output of MapQTL. A_f is female additivity, i.e., the average effect of substituting one female allele for the other (b → a) and A_m is male additivity, i.e., the average effect of substituting one male allele for the other (d → c). D is the overall dominance effect, i.e., the deviation from additivity, where a value of zero indicates complete additivity. To compare the degrees of the allelic effects between traits with different scales of variance, the allelic effects were standardized by dividing by the standard deviation (SD) of the trait. The relative size of female and male additivity was characterized as the ratio of their absolute values $|A_f|/|A_m|$. The relative size of dominance effect against additivity was characterized as $|2D|/(|A_f| + |A_m|)$.

Results

Genetic variability of traits

The 98 F_1 genotypes were divided into 32 recurrent blooming and 66 non-recurrent blooming genotypes. The recurrent blooming characteristic is controlled by a single recessive locus *RB*, *RECURRENT BLOOMING* (e.g., Semeniuk 1971a, b; De Vries and Dubois 1984; Debener 1999; Hibrand-Saint Oyant et al. 2008). The ratio of 32 and 66 hybrids differed significantly from the expected ratio of 1:1 ($\chi^2 = 6.12$, $P < 0.05$).

Genotypic LS-means of the date of first flowering (*D1Flower*) ranged from 6.9 to 31 days among 98 F_1 progenies (Table 1). The two parents bloomed on an average of 17.5 and 13.6 days, respectively, at similar periods, indicating transgressive segregation. About 57% of total phenotypic variance (σ^2_P) of *D1Flower* was attributed to genetic variance (σ^2_G), and broad-sense heritability (h^2) was estimated at 0.92 (Table 1). The genotype × year interaction (σ^2_{GY}) was significant ($P < 0.05$) but was relatively small (8.8%). The relative ranks of *D1Flower* among the 98 genotypes were well conserved over the four-year study period (Supplementary data, Fig. 1S).

The ranges of inflorescence trait values of F_1 hybrids were generally beyond the values of the two parents, indicating transgressive segregation (Table 1). The percentages of σ^2_G ranged 33–63% of σ^2_P, indicating substantial genetic variability of inflorescence architecture. The high h^2, ranging 0.82–0.93 (average 0.9) demonstrated that the genetic analyses of the inflorescence architecture of this population were reliable. The σ^2_{GY} components were not significant in any inflorescence traits ($P > 0.05$). The average trait values obtained for each genotype in each year were highly correlated between the 2 years (r ranged 0.64–0.86, average 0.76, $P < 0.0001$), and the relative ranks of genotypic means were well conserved (Supplementary data, Fig. 2S). Variance between replicated plants within a genotype (σ^2_R) ranged from 13 to 31% (average 19%), and variance in the length of internodes *LV1-LF1-LF2* tended to be large (21–31%). Residual error variance (σ^2_E), which was attributed to within-plant variation and measurement error, was generally greater than σ^2_R and ranged from 21 to 48% (average 33%).

Correlation among traits

Recurrent blooming habit was weakly correlated with early flowering. The genotypic LS-means of *D1Flower* averaged 16.3 and 21.1 day for recurrent blooming and non-recurrent blooming genotypes, respectively, and these were significantly different ($F_{1,96} = 18$, $P < 0.0001$; Supplementary data, Table 1S). However, the ranges of genotypic LS-means of *D1Flower* largely overlapped, 6.9–27.7 days for recurrent blooming genotypes and 10.2–31.8 days for non-recurrent blooming genotypes.

Table 2 shows genotypic correlations (r_g) between flowering time and inflorescence traits. *D1Flower* was significantly correlated with inflorescence traits ($P < 0.001$), except for the number of inflorescence nodes, *NF1* and *NF2* ($P > 0.05$). Late flowering genotypes produced more number of vegetative nodes (*NV1*), shorter internodes (*LV1*, *LF1*, and *LF2*), less number of 3rd order shoots (*NBF2*) and branching intensity (*BIF2*) of 2nd order shoot of inflorescence part and less number of flowers (*FLW*) than early flowering genotypes.

On the other hand, both strong ($r > 0.7$) and weak (non-significant) correlations were found among inflorescence traits (Table 2; See also Fig. 3b). Number of flowers (*FLW*) was the most highly correlated with number of 3rd order shoots of inflorescence part (*NBF2*) ($r_g = 0.88$) because of the direct effect of branching on flower production. By definition (Fig. 1), *NBF2* was the product of the number of nodes (*NF2*) and branching intensity (*BIF2*). Both *NF2* and *BIF2* were highly correlated with *NBF2*, whereas they were not significantly correlated with each other ($r_g = -0.2$, $P > 0.05$). Thus, there were two independent developmental pathways associated with the variations in *NBF2* and hence *FLW*: one pathway was related to node production (*NF2*) and the other was with axillary branching (*BIF2*). Number of nodes on 2nd order shoot of inflorescence part (*NF2*) was highly correlated with that of 1st order shoot (*NF1*) ($r_g = 0.86$, $P < 0.001$), whereas neither *NF1* nor *NF2* was significantly correlated with the length of internodes, *LF1* or *LF2* ($P > 0.05$). In

Table 2 Genotypic (r_g) correlation coefficients between flowering time and 9 inflorescence traits in a population of 98 F_1 hybrids derived from the cross *TF* × *RW*

	D1Flower	Log (*NV1*)	*NF1*	*NF2*	*LV1*	*LF1*	*LF2*	*NBF2*	Log (100 − *BIF2*)
Log (*NV1*)	0.66***								
NF1	0.04^{ns}	−0.07^{ns}							
NF2	0.01^{ns}	−0.04^{ns}	0.86***						
LV1	−0.28***	0.02^{ns}	0.06^{ns}	−0.10^{ns}					
LF1	−0.61***	−0.51***	0.14^{ns}	0.01^{ns}	0.64***				
LF2	−0.69***	−0.44***	0.00^{ns}	−0.08^{ns}	0.65***	0.82***			
NBF2	−0.45***	−0.31**	0.67***	0.70***	0.26**	0.42***	0.49***		
Log (100 − *BIF2*)	0.64***	0.41***	−0.27**	−0.20^{ns}	−0.48***	−0.60***	−0.77***	−0.82***	
Sqrt (*FLW*)	−0.56***	−0.31**	0.51***	0.51***	0.36***	0.48***	0.65***	0.88***	−0.87***

Pearson's product-moment coefficients were calculated by genotypic least-square means

D1Flower (date when once the petals are visible under the sepals), *NV1* (number of nodes on *VEG1*, vegetative part of 1st order shoot), *NF1* (number of nodes on *INF1*, inflorescence part of 1st order shoot), *NF2* (number of nodes on *INF2*, the longest 2nd order shoot of the inflorescence), *LV1* (average internode length of *VEG1*), *LF1* (average internode length of *INF1*), *LF2* (average internode length of *INF2*), *NBF2* (number of 3rd order shoots of *INF2*), *BIF2* (percentage of lateral meristems on *INF2* which develop into 3rd order shoots), *FLW* (total number of flowers produced by *INF1*)

^{ns} $P > 0.05$; * $P < 0.05$; ** $P < 0.01$; *** $P < 0.001$

contrast, branching intensity of 2nd order shoot (*BIF2*) was highly correlated with *LF2* ($r_g = 0.77$, $P < 0.001$) and *LF1* ($r_g = 0.60$, $P < 0.001$), and *LF1* was highly correlated with *LF2* ($r_g = 0.82$, $P < 0.001$). Thus, the two independent variations in inflorescence architecture can be summarized as follows: (1) The increase in the production of nodes in the inflorescence (*NF1* and *NF2*) led to an increase in the number of 3rd order shoots and in the total number of flowers (*NBF2* and *FLW*), and (2) the longer internode elongation (*LF1* and *LF2*) was linked with higher branching frequency (*BIF2*) and increased *NBF2* and *FLW* (Fig. 3b; See also schematic illustrations in Fig. 3S).

Vegetative characteristics were relatively independent of reproductive characteristics. Number of nodes on 1st order shoot of vegetative part (*NV1*) was not correlated with that of inflorescence part (*NF1*) ($r_g = -0.07$, $P > 0.05$), although length of vegetative internodes (*LV1*) was significantly correlated with that of inflorescence internodes (*LF1*) ($r_g = 0.64$, $P < 0.001$).

Genetic linkage map

We used 55 and 70 markers to construct the genetic linkage map of *TF* and *RW*, respectively. The map of *TF* covers 391.1 cM, and the map of *RW* covers 406.9 cM. Both maps were divided into seven LGs corresponding to the seven rose chromosomes, and each LG contains 5–10 bi-parental markers (i.e., common markers). Homologous linkage groups were then combined to build an integrated map (Fig. 2). The numbers of the LGs were assigned according to the maps of Hibrand-Saint Oyant et al. (2008) using the common markers. The integrated map covers 403 cM with the average marker density of 5.4 cM/marker. The largest gap was 26 cM in LG7. A significant distortion of marker segregation from the expected Mendelian segregation was observed in several markers. Strong distortions (***$P < 0.001$) were identified for the *TF* alleles on LG3 (2–11 cM from the top) and for the *RW* alleles around locus *RB* on LG4 (31–56 cM) and in part of LG7 (0–18 cM).

QTL analysis

The *RB* locus was mapped on LG4 in a region with a strong distortion (Fig. 2). Perfect co-localization was detected with *RoKSN*, the gene controlling recurrent blooming (unpublished results from our laboratory). For 10 inflorescence developmental traits, a total of 31 QTLs was identified (Table 3), and most of them were clustered into six specific chromosomal regions (cQTL, Fig. 3a). The detailed locations of QTLs are presented in supplementary data (Fig. 4S).

Three significant QTLs were detected for *D1Flower*, which accounted for a total of 51.5% of σ^2_P and 56% of σ^2_G (Table 3). A major QTL, *D1Flw-1* (LOD = 12.8; $r^2 = 28\%$) co-localized with *RoFT*, a homologue of *Arabidopsis* flowering integrator, *FT* (Remay et al. 2009) on LG3 (Fig. 3). The second QTL, *D1Flw-2* with a marked effect (LOD = 7.2; $r^2 = 14.5\%$) was mapped on LG4. In the vicinity of this QTL, four genes involved in floral initiation were mapped: *RoVIP3*, a homologue of *Arabidopsis* flowering repressor, *VERNALIZATION INDEPENDENCE 3* (Foucher et al. 2008), homologues of genes involved in GA signaling (*RoSPINDLY* and *RoDELLA*; Remay et al.

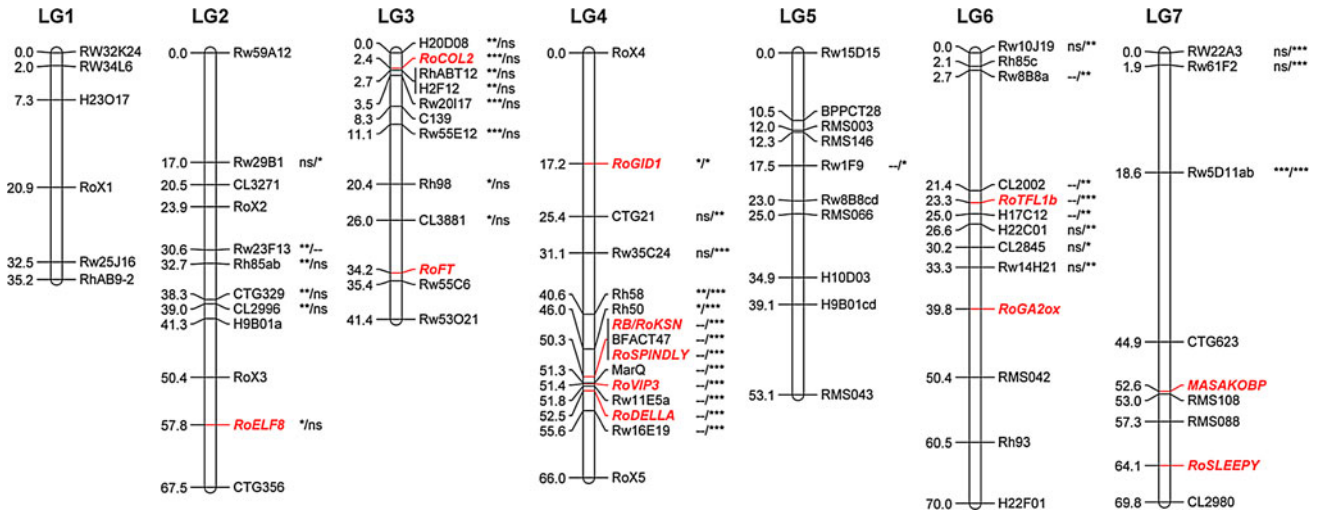

Fig. 2 Integrated linkage map of 98 F_1 diploid roses obtained from the cross The Fairy (*TF*) × a hybrid of *R. wichurana* (*RW*). Marker names are shown to the *right* of each LG. Genes are in *bold italics*. Distances (Kosambi cM) are given on the *left*. Marker segregation distortion was tested against the expected Mendelian ratios using the chi-square test, and distortion was tested for *TF* and *RW* alleles separately. Marker segregation distortions are indicated on the right of the marker for *TF*/*RW* alleles (ns $P > 0.05$; *$P < 0.05$; **$P < 0.01$; ***$P < 0.001$; – no segregation because of uni-parental marker)

2009), and *RB*/*RoKSN*. An additional minor QTL, *D1Flw-3* (LOD = 4.9; $r^2 = 9\%$) was found on LG7. For *D1Flw-1* and *D1Flw-3*, both female and male allelic effects (A_f, A_m) were substantial, indicating both *TF* and *RW* were heterozygous at these QTLs. In contrast, A_f of *D1Flw-2* was small, suggesting that *TF* is homozygous at this locus.

For nine inflorescence traits, we detected two to four significant QTLs per trait (Table 3). Most QTLs had marked effects with $r^2 > 10\%$ (up to 42%). The percentages of σ^2_P and σ^2_G explained by all significant QTLs (i.e., R^2 and R^2/h^2) ranged from 51 to 70% and 59 to 76%, respectively. From the significant QTLs for inflorescence traits, five common regions (cQTL) were identified (Fig. 3a). All inflorescence traits, except for *LV1*, had a significant QTL in the cQTL3 located near *RoFT* on LG3. The r^2 of inflorescence QTLs in this region was always greater than 16% (up to 42% for *NV1-1*), indicating the presence of a major QTL controlling overall inflorescence architecture.

The cQTL4 of LG4 contained several major QTLs, *LV1-1* (LOD = 15.5, $r^2 = 33\%$), *LF2-1* (LOD = 9.6, $r^2 = 28\%$), *BIF2-1* (LOD = 8.5, $r^2 = 25\%$), and *FLW-2* (LOD = 9.1, $r^2 = 21\%$). The cQTL4 controlled *FLW* by affecting the internode elongation (*LF2*, *LF1*) and branching intensity (*BIF2*) of the inflorescence (Fig. 3b). The levels of A_f by the QTLs in cQTL4 were null compared to A_m (Table 3), indicating that *TF* is homozygous at these QTLs. The cQTL4 was located near the *RB*/*RoKSN*, *RoSPINDLY*, and *RoDELLA* (Fig. 3a).

The cQTL1 located on the upper arm of LG1 affected node production (*NV1*, *NF1*, *NF2*). In particular, major QTLs for inflorescence node production, *NF1-2* (LOD = 8.2, $r^2 = 22\%$) and *NF2-1* (LOD = 8.9, $r^2 = 29\%$), were located in this region. The *NBF2* and *FLW* also had significant QTLs (*NBF2-3* and *FLW-3*). The *NBF2* and *FLW* were affected by cQTL1 through its control of node production (*NF1*, *NF2*) in the inflorescence (Fig. 3b). The similar magnitudes of A_f and A_m suggest that both parents are heterozygous at the locus.

Relatively minor but substantial QTLs ($r^2 = 10$–20%) were detected in cQTL2 on LG2 and cQTL5 on LG5. The cQTL2 contained QTLs affecting node production of 1st order shoots (*NV1-2* and *NF1-3*). One putative candidate gene, *RoELF8*, a homologue of the flowering repressor gene in *Arabidopsis* (Foucher et al. 2008), was located near cQTL2 (Fig. 3). In LG5, QTLs for internode elongation (*LV1-2*, *LF1-1*, *LF2-3*), node production (*NV1-4*), and branch number (*NBF2-4*) were identified (Table 3). The three QTLs for internode elongation co-localized with similar allelic effects (i.e., their A_f and A_m were all negative). We therefore concluded that the three QTLs (*LV1-2*, *LF1-1*, *LF2-3*) were a potentially common QTL, cQTL5 (Fig. 3a). The two QTLs *NV1-4* and *NBF2-4* were located at a slight small distance from cQTL5, and so we did not include them in cQTL5.

A minor QTL, *LV1-4* (LOD = 4.0, $r^2 = 7\%$) controlling internode elongation of the vegetative parts was identified in the region of cQTL7 on LG7 (Fig. 3a), where the flowering QTL *D1Flw-3* was also located (Table 3). cQTL7 co-localized with *RoSLEEPY*, a homologue of *Arabidopsis SLEEPY* gene (Foucher et al. 2008), which regulates GA signaling in *Arabidopsis*. On LG6, no significant QTLs were detected in this study.

Table 3 QTL for flowering time and inflorescence traits, estimated from genotypic least-square means of 98 F_1 hybrids derived from the cross *TF* × *RW*

Trait[g]	QTL	LOD[a]	QTL position			Cofactor[c]	Allelic effect[d]					PVE[e]		
			LG	cM	Interval[b]		A_f	A_m	D	(A_f/A_m)	(D/A)	r^2	R^2	(R^2/h^2)[f]
D1Flower	*D1Flw-1*	12.79 (3.7)	LG3	35	31–35 (28–35)	*RoFT*	1.08	−1.95	−0.55	0.56	0.36	28	51.5	0.56
	D1Flw-2	7.22 (3.7)	LG4	56	52–66 (51–66)	Rw16E19	−0.25	−1.65	−0.64	0.15	0.67	14.5		
	D1Flw-3	4.92 (3.7)	LG7	53	51–57 (51–57)	RMS108	0.96	0.99	0.43	0.97	0.44	9		
Log (*NV1*)	*NV1-1*	22.28 (3.8)	LG3	35	32–35 (32–35)	*RoFT*	1.65	−2.23	−0.48	0.74	0.25	42.1	70.8	0.76
	NV1-2	9.13 (3.8)	LG2	41	38–45 (38–47)	H9B01a	−0.47	−1.52	−0.15	0.31	0.15	12.1		
	NV1-3	7.25 (3.8)	LG1	1	0–2 (0–2)	Rw32K24	−1.10	−0.82	0.15	1.35	0.15	9.4		
	NV1-4	5.31 (3.8)	LG5	29	24–35 (23–39)	H10D03	0.93	0.70	−0.04	1.34	0.05	7.2		
NF1	*NF1-1*	9.23 (3.7)	LG3	34	31–35 (28–35)	*RoFT*	−1.24	0.42	1.41	2.99	1.71	24	59.3	0.65
	NF1-2	8.2 (3.7)	LG1	6	0–8 (0–8)	Rw34L6	−1.11	−1.68	0.14	0.66	0.10	22.2		
	NF1-3	4.41 (3.7)	LG2	50	42–55 (41–58)	RoX3	−1.21	−0.54	0.52	2.26	0.60	13.1		
NF2	*NF2-1*	8.99 (3.7)	LG1	6	0–8 (0–8)	Rw34L6	−1.21	−1.95	0.16	0.62	0.10	28.7	54.2	0.60
	NF2-2	8.64 (3.7)	LG3	34	26–35 (25–35)	*RoFT*	−1.88	0.43	0.56	4.38	0.49	25.5		
LV1	*LV1-1*	15.53 (3.7)	LG4	50	48–50 (47–50)	*RoKSN*	−0.15	2.48	−0.31	0.06	0.23	33.1	61.4	0.75
	LV1-2	6.56 (3.7)	LG5	39	37–43 (36–45)	H9B01cd	−1.22	−0.97	−0.43	1.26	0.40	11.1		
	LV1-3	6.03 (3.7)	LG1	2	0–8 (0–8)	RW34L6	−0.82	0.79	−0.52	1.04	0.65	10.2		
	LV1-4	4.03 (3.7)	LG7	65	60–70 (57–70)	*RoSLEEPY*	−0.82	−0.67	0.05	1.23	0.06	7		
LF1	*LF1-1*	8.3 (3.8)	LG5	39	36–44 (35–47)	H9B01cd	−1.63	−1.29	−0.74	1.26	0.51	19.2	53.9	0.61
	LF1-2	8.16 (3.8)	LG3	34	29–35 (26–35)	*RoFT*	−1.31	1.10	0.71	1.20	0.59	19.1		
	LF1-3	6.47 (3.8)	LG4	48	46–50 (45–50)	*RoKSN*	−0.02	1.64	−0.18	0.01	0.21	15.6		
LF2	*LF2-1*	9.61 (3.8)	LG4	48	46–50 (46–50)	*RoKSN*	−0.26	2.19	−0.31	0.12	0.25	28.4	55.4	0.63
	LF2-2	6.19 (3.8)	LG3	34	28–35 (25–35)	*RoFT*	−0.26	1.63	0.38	0.16	0.41	16.3		
	LF2-3	4.21 (3.8)	LG5	39	35–44 (34–47)	H9B01cd	−0.73	−1.30	−0.56	0.56	0.55	10.7		
NBF2	*NBF2-1*	9.82 (3.7)	LG3	34	25–35 (25–35)	*RoFT*	−1.13	1.41	0.92	0.80	0.73	21.4	57.7	0.68
	NBF2-2	8.04 (3.7)	LG4	48	46–50 (46–50)	*RoKSN*	−0.22	1.78	−0.01	0.12	0.01	17.2		
	NBF2-3	5.29 (3.7)	LG1	0	0–2 (0–2)	RW32K24	−0.68	−1.16	0.42	0.59	0.46	10.1		
	NBF2-4	3.82 (3.7)	LG5	30	25–38 (24–39)	H10D03	1.21	−0.41	−0.07	2.99	0.09	9		
Log (100-*BIF2*)	*BIF2-1*	8.56 (3.8)	LG4	50	47–50 (46–50)	*RoKSN*	−0.16	−2.13	0.00	0.08	0.00	25.3	50.5	0.59
	BIF2-2	8.54 (3.8)	LG3	34	27–35 (25–35)	*RoFT*	0.37	−1.87	−0.90	0.20	0.80	25.2		
Sqrt (*FLW*)	*FLW-1*	10.99 (3.9)	LG3	34	26–35 (25–35)	*RoFT*	−0.71	1.84	0.88	0.38	0.69	26.7	58.1	0.63
	FLW-2	9.13 (3.9)	LG4	50	47–50 (46–50)	*RoKSN*	−0.08	1.94	−0.18	0.04	0.17	21.3		
	FLW-3	4.87 (3.9)	LG1	0	0–2 (0–2)	RW32K24	−0.59	−1.09	0.58	0.54	0.69	10.1		

[a] Maximum LOD score with threshold LOD in parenthesis

[b] 1-LOD interval cM with 2-LOD interval cM in parenthesis

[c] Markers used as cofactors for MQM mapping procedure

[d] Allelic effect calculated based on estimated phenotypic value, u_{ac}, u_{ad}, u_{bc}, u_{bd} associated with each of the 4 possible genotypic classes, ac, bc, ad, and bd, deriving from the cross ab (female) × cd (male). A_f is female additivity calculated as $[(u_{ac} - u_{bc}) + (u_{ad} - u_{bd})]/(2SD)$, A_m is male additivity calculated as $[(u_{ac} - u_{ad}) + (u_{bc} - u_{bd})]/(2SD)$, and D is the overall dominance effect calculated as $[(u_{ac} + u_{bd}) - (u_{ad} + u_{bc})]/(2SD)$. Values are standardized by dividing by the standard deviation (SD) of the trait. (A_f/A_m) is the relative effect of female/male additivity calculated as A_f/A_m, and (D/A) is the relative effect of dominance/additivity calculated as $2D/(A_f + A_m)$

[e] Percentage of phenotypic variance explained by each QTL (r^2) and by all significant QTLs (R^2) in each trait

[f] Proportion of genetic variance explained by QTLs calculated by dividing R^2 by broad-sense heritability (h^2, %)

[g] *D1Flower* (date when once the petals are visible under the sepals), *NV1* (number of nodes on *VEG1*, vegetative part of 1st order shoot), *NF1* (number of nodes on *INF1*, inflorescence part of 1st order shoot), *NF2* (number of nodes on *INF2*, the longest 2nd order shoot of the inflorescence), *LV1* (average internode length of *VEG1*), *LF1* (average internode length of *INF1*), *LF2* (average internode length of *INF2*), *NBF2* (number of 3rd order shoots of *INF2*), *BIF2* (percentage of lateral meristems on *INF2* that develop into 3rd order shoots), *FLW* (total number of flowers produced by *INF1*)

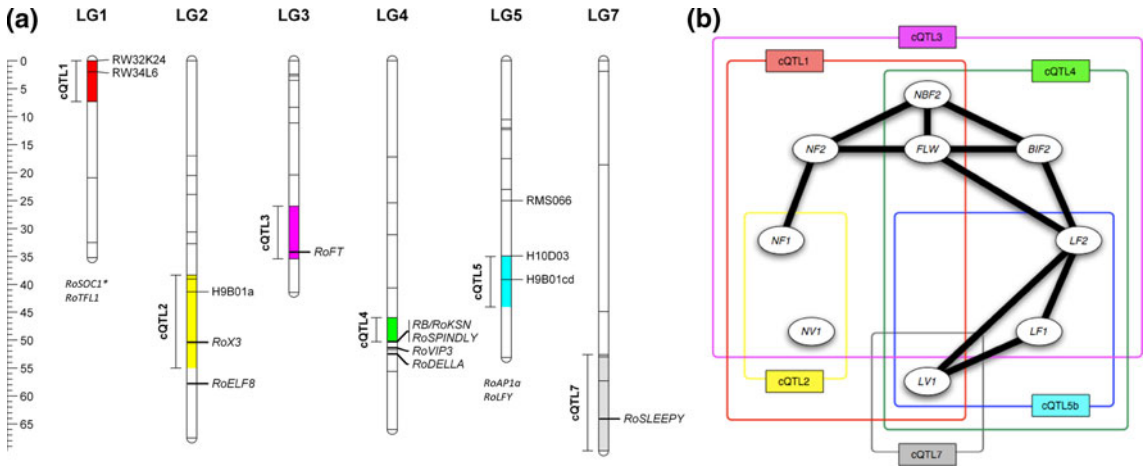

Fig. 3 **a** Common genomic regions of QTL for 10 inflorescence developmental traits detected by MQM mapping in 98 F_1 diploid roses derived from the cross The Fairy (*TF*) × a hybrid of *R. wichurana* (*RW*). *Left bar* shows the map scale in cM. QTLs for different traits with overlapping confidence intervals (1-LOD) were declared to be common QTLs (cQTL). The regions of cQTL and the names of markers used as cofactors and putative candidate genes are shown. *Asterisk* indicates putative candidate genes mapped by Remay et al. (2009) are also indicated at the bottom of each LG. **b** Diagram summarizing the genotypic correlations between inflorescence traits and the cQTLs controlling these traits. Highly correlated traits ($|r_g| > 0.6$, $P < 0.001$) are connected by *thick lines*. *NV1*, number of nodes on vegetative part of 1st order shoot (*VEG1*); *NF1*, number of nodes on inflorescence part of 1st order shoot (*INF1*); *NF2*, number of nodes on the longest 2nd order shoot of inflorescence (*INF2*); *LV1*, average internode length of *VEG1*; *LF1*, average internode length of *INF1*; *LF2*, average internode length of *INF2*; *NBF2*, number of 3rd order shoots of *INF2*; *BIF2*, Percentage of lateral meristems on *INF2* which develop into 3rd order shoots; *FLW*, total number of flowers produced by *INF1*

Discussion

Genetic variability and modes of inheritance

Recurrent blooming characteristic is controlled by a single recessive locus *RB* (e.g., Semeniuk 1971a, b; De Vries and Dubois 1984; Debener 1999; Hibrand-Saint Oyant et al. 2008). However, the ratio of 32 recurrent blooming and 66 non-recurrent blooming genotypes differed significantly from the expected ratio of 1:1. This can be explained by the presence of a gametophytic *SI*-locus linked to *RB* (Spiller et al. 2010b) which is strengthened by the presence of large distortions observed in the male markers linked to *RB* (Fig. 2).

Broad-sense heritability at the genotypic mean level (h^2) has been used as an index of reliability of phenotypic selection for genetic characteristics (Holland et al. 2003), and the accuracy of QTL analysis largely depends on the level of h^2 (Beavis 1998). We demonstrated that in our mapping population, h^2 of flowering time and inflorescence traits were sufficiently high (>0.8) to enable genetic analyses of these characteristics. We also showed that the percentage of genetic variance (σ^2_G) in total phenotypic variance (σ^2_P) was low to moderate (32–62%). Therefore, the single measurement of an individual or a shoot is not enough to characterize the genotype, and repeated measurements are necessary to reduce non-genetic noise. The non-genetic variance components were mainly due to within-plant variability (σ^2_E) rather than to between-plant variability (σ^2_R), indicating that in our population, the increased repetition of shoots rather than of individuals is a more efficient phenotyping strategy to increase the accuracy of phenotypic evaluation of inflorescence characteristics. Furthermore, genotypic correlations were significant for most (78/90) pairs of traits (Table 2). Therefore in our segregating population, phenotyping of inflorescence traits can be simplified by scoring only a few traits (i.e., non-correlated traits, Table 2; Fig. 3b). For inflorescence traits, the scoring of *FLW* (total number of flowers produced), *NF* (number of inflorescence nodes) and *LF* (length of internodes) is sufficient for a description of the inflorescence.

Our morphological dissection of complex inflorescence architecture clarified several distinct rules in the inheritance of rose inflorescence architecture. The *NF* of 1st order shoots (*NF1*) was tightly correlated with that of 2nd order shoots (*NF2*), and they did not segregate independently. Tight correlations were also observed between *LF1*-*LF2* and *LF*-*BIF2* (Table 2). Consequently, inflorescence types observed in the population were restricted to a limited range of possible types (Fig. 3S, a–b for schematic illustrations). In contrast, *NF* and *LF* were not significantly correlated (Table 2), allowing the inflorescence types segregated over the two-dimensional 'morphospace' (see Prusinkiewicz et al. 2007) defined by the diagonal axes of these traits (Fig. 3S, c). Since the increase in *LF* was coupled with increasing *BIF2*, the developmental pathways determining the *FLW* were separated into two pathways related to *NF* and *LF* (Fig. 3b).

Genetic linkage map

Our new genetic linkage map spanned a total of 403 cM, which is comparable to previously reported maps of diploid roses (reviewed by Debener and Linde 2009), and was expected to cover a large part of the rose genome. Statistical estimation of the genome coverage performed by repeated sampling of the markers mapped on diploid roses indicated that the total length of the rose genome was approximately 500 cM (Yan et al. 2005). A few zones of the genome present markers with a high distortion (Fig. 2). The marker distortion on LG2 and LG3 were concentrated on female alleles, indicating the possibility of pre-zygotic selection of female gametes (e.g., Crespel et al. 2002; Hibrand-Saint Oyant et al. 2008). In contrast, the distortions in LG4 were concentrated on male alleles, which may be at least partly due to the presence of a gametophytic *SI*-locus (Spiller et al. 2010b).

QTL analysis

The present study clearly demonstrated polygenic control of flowering time and inflorescence architecture in rose. However, the small population size (<100 individuals in our study) may have caused several biases in the estimates of the QTL analysis. Beavis's simulation study showed that if the population was small (e.g., 100 progeny), the estimated number of QTLs was biased downwards, and the estimates of σ_P^2 explained by the detected QTL was biased upwards (Beavis 1998). The "Beavis effect" was also confirmed by a theoretical analysis (Xu 2003). Our analysis showed that most QTLs were of large effects ($r^2 > 10\%$), and the percentages of σ_G^2 explained by all significant QTLs (R^2/h^2) were 59–76%. It appears that, like the Beavis effect, many minor QTLs may be undetected, and the r^2 of the detected QTLs may be overestimated in our study. Further studies using a large population are required to identify minor QTLs and to obtain the precise estimates of QTL effects.

A few studies have been conducted on QTLs for flowering time in rose (Dugo et al. 2005; Hibrand-Saint Oyant et al. 2008). Hibrand-Saint Oyant et al. (2008) detected a strong QTL (*BD*, LOD = 6.38; $r^2 = 34\%$) co-localized with the *RB* locus on LG4. The *BD* and *D1Flw-2* are potentially the same locus. Dugo et al. (2005) reported two significant QTLs for flowering time in a different population in Spain, but a comparison is impossible since the homology of linkage group is currently unknown.

Clustering of QTLs was clear and consistent with strong genetic correlations among inflorescence developmental traits: a large proportion of QTLs had overlapping 2-LOD support intervals and were clustered in six specific chromosomal regions (i.e., cQTL1, 2, 3, 4, 5, and 7; Fig. 3a). It was not possible to determine whether these patterns result from pleiotropic effects of single genes or tight linkage, however, co-localizations with candidate genes were found for a few of these QTLs.

Candidate genes and QTL co-localization

TFL1/FT gene family

The *TFL1/FT* is a multigenic family whose members are involved in flowering. In *Arabidopsis thaliana*, *FT* is a floral integrator that promotes flowering, whereas *TFL1* represses the transition (Kobayashi et al. 1999). *FT* protein, which was demonstrated to be a component of florigen, travels via the phloem from the leaf to the SAM, where, through interactions with additional proteins, it activates floral transition (see Turck et al. 2008 for a review). In contrast, *TFL1* is expressed in shoot apical meristem and plays a role in the maintenance of meristem indeterminacy. In *Arabidopsis*, overexpression of *TFL1* delays flower formation and forms a highly branched inflorescence, whereas *tfl1* mutants have a short vegetative phase and form a simple determinate inflorescence with a terminal flower (Bradley et al. 1997). The structure and function of *TFL1/FT* genes are greatly conserved in plants. Overexpression of *FT* orthologues in transgenic plants from several species, including woody perennial plants such as poplar (Böhlenius et al. 2006), resulted in precocious flowering (see Jung and Müller 2009 for a review).

We showed that a major QTL for flowering time co-localized with *RoFT*, a *FT* homologue in rose (Remay et al. 2009). The *RoFT* transcripts accumulated in rose apices during the period of floral initiation (Remay et al. 2009). These results strongly indicate that *RoFT* is a putative candidate gene controlling flowering time in rose. The QTLs for many inflorescence traits also co-localized with *RoFT*, possibly due to its pleiotropic effects. The delay in floral initiation of the terminal apex increased *NV1* but decreased *NF1*, and consequently, late flowering genotypes formed simpler inflorescences than early flowering ones. The co-localizations of *FT*-like genes and the QTLs for flowering time have been reported in domesticated rice (Kojima et al. 2002; Hagiwara et al. 2009), wheat (Yan et al. 2006; Bonnin et al. 2008), barley (Kikuchi et al. 2009; Wang et al. 2010), and sunflower (Blackman et al. 2010).

Recently, in our laboratory, the *RECURRENT BLOOMING* gene was demonstrated to be a *TFL1* homologue, *RoKSN*. In the present study, cQTL4 including the QTL for flowering time and inflorescence architecture was mapped near *RoKSN* (Fig. 3a). Non-recurrent blooming hybrids (*KSN/ksn*) showed significantly later flowering time and less elongated and branched inflorescences than recurrent blooming hybrids (*ksn/ksn*) (Table 1S). This appears to agree with the function of *RoKSN* as flowering

repressor. *RoKSN* may affect flowering time and inflorescence architecture in rose. Furthermore, another member of the *TFL1* family, *RoTFL1*, was located on LG1 (Remay et al. 2009). On this LG, we showed the presence of cQTL1. Mapping of *RoTFL1* is in progress. cQTL1 controls inflorescence node production, whereas cQTL4 regulates the flowering time and branching frequency of the inflorescence (Fig. 3a), indicating a functional differentiation in these loci. The differential expression and function of *TFL1* paralogues have been reported in several plants, such as pea (Foucher et al. 2003), Rosaceae fruit trees (Esumi et al. 2008; Mimida et al. 2009), and barley (Kikuchi et al. 2009). Testing the functional differentiation of *RoTFL1* and *RoKSN* is planned.

Overall, we suggest that at least two (and possibly three) genes of the *TFL1*/*FT* family are involved in the control of floral transition and inflorescence development in rose. This family was first described as involved only in phase transition in the annual plant *Arabidopsis thaliana* (Kobayashi et al. 1999), however recent studies revealed a more general role in plant development, and the *TFL1*/*FT* family has been shown to regulate reiterative growth and flowering cycles in perennial plants, such as poplar (Böhlenius et al. 2006) and tomato (Shalit et al. 2009). The agronomic importance of the *TFL1*/*FT* family was also emphasized by recent works that identified artificial selections in *TFL1*/*FT* genes in a wide range of domesticated plants, including sunflower (Blackman et al. 2010) and soybean (Tian et al. 2010). In tomato, this family was shown to greatly affect total yield (Krieger et al. 2010).

GA related genes (DELLA, SPINDLY, and SLEEPY):

The genomic region of cQTL4 also contained other candidate genes, *RoVIP3*, *RoDELLA*, and *RoSPINDLY*, which may be involved in the control of floral initiation in rose (Remay et al. 2009). In particular, *RoSPINDLY* and *RoDELLA* rather than *RoKSN* are likely candidate genes for QTLs of inflorescence internode elongation (*LF1* and *LF2*). GA is known to influence internode elongation in rose (Roberts et al. 1999) as shown in many plants. *DELLA* proteins are negative regulators of GA signaling in *Arabidopsis* (Dill et al. 2001), and their functions are well conserved in plants (Harberd et al. 2009). *SPINDLY* encodes an *O*-linked *N*-acetylglucosamine (GlcNAc) transferase and is thought to activate *DELLA* proteins (Silverstone et al. 2007). Given the high degree of similarity between *RoDELLA* and *RoSPINDLY* and their putative orthologues in *Arabidopsis* (Foucher et al. 2008; Remay et al. 2009), it is likely that the genes perform similar functions in rose, and may be good candidates for cQTL4. Furthermore, a QTL for internode length of vegetative part (*LV1-4*) on LG7 co-localized with *RoSLEEPY*, a homologue of the *Arabidopsis* gene, which encodes a putative F-box protein and positively regulates GA signaling (Steber et al. 1998). Further experimental studies by exogenous GA-application will elucidate the involvement of GA in determining these traits in rose.

Floral identity genes (LFY and AP1)

The *LFY* and *AP1* encode transcription factors and are required for the activation of floral meristem identity genes in *Arabidopsis* (reviewed by Krizek and Fletcher 2005). *Arabidopsis lfy* and *ap1* mutants formed compound inflorescence architectures by converting lateral flowers into secondary inflorescence shoots. In rose, the transcript accumulation of *RoLFY* and *RoAP1a* increased in shoot apices during the floral process (Remay et al. 2009), as previously shown in *Arabidopsis*, suggesting their involvement in floral transition. *RoLFY* was mapped between two SSRs, H10D03 and H9B01cd, and *RoAP1a* was located on 7.6 cM lower position from H9B01cd in HW map (Remay et al. 2009), indicating that these genes are located in the 1-LOD interval of cQTL5 (Fig. 3a). They are thus possible candidate genes controlling inflorescence architecture in rose. Further mapping studies and a more detailed spatiotemporal expression analysis are necessary to test their functions.

Other genes

In *Arabidopsis*, the inputs from the vernalization and photoperiod pathways are integrated by flowering pathway integrators, *FT* and *SOC1* (Parcy 2005). *SOC1* encodes a MADS box protein and is well conserved in Angiosperms (see Lee and Lee 2010 for a review). Remay et al. (2009) isolated *RoSOC1*, a rose orthologue of *SOC1*, and mapped it on LG1. Since node production is largely determined by the timing of floral induction, *RoSOC1* may be also another candidate gene for cQTL1. Localization of floral organ identity genes, *MASAKO B3*, *MASAKO C1*/*RAG*, and *MASAKO BP* (homologues of *Arabidopsis APETALA3*, *AGAMOUS*, *PISTILLATA*, respectively; Kitahara and Matsumoto 2000; Kitahara et al. 2001) were determined by Remay et al. (2009) and in this study, whereas no co-localization of these genes with inflorescence QTLs was found. It should be also noted that many other possible candidate genes which have been shown to affect inflorescence architecture (see Bhatt 2005 for a list of inflorescence development mutants of model plants), remain untested.

Conclusions

The present study quantified the genetic variability of inflorescence developmental traits in a F_1 diploid rose

population by intensive measurements of phenological and morphological traits in the field. QTL analysis identified several genomic regions controlling these traits. The results demonstrated that flowering time and many inflorescence traits were controlled by common genomic regions. However, morphological dissection of inflorescence architecture identified several developmental components (e.g., node production, internode elongation, and axillary branching) that were controlled by separate genomic regions. These modes of inheritance and their underlying genetic architecture may act as a constraint on the breeding potential for the size and design of the inflorescence in rose. The strong genotypic correlations prevent independent selection of these traits, although the low correlations result in a diversity of inflorescence architecture by allowing the independent inheritance of the traits. Nevertheless, the patterns of inheritance are necessarily restricted to the genetic variation segregating between parents, and the population represents only a small fraction of the global diversity in rose. Therefore, a more comprehensive analysis of genetic architecture is required based on multiple populations representing a larger sample of the standing genetic variation in rose. We also identified several flowering genes that are plausible candidate genes for the control of inflorescence development in rose. These can be pursued through finer-scale mapping, sequence analysis, expression analysis, physiological study, and/or association mapping.

Acknowledgments We thank Drs. Evelyne Costes, Vincent Segura, Damien Fumey (INRA Montpellier), Patrick Favre, Philippe Morel, and Gilles Galopin (SAGAH, INRA Angers) for their helpful advice on plant measurements, Charles-Eric Durel, Sylvain Gaillard, Fabrice Dupuis, and Alix Pernet (GenHort, INRA Angers) for statistical analyses, Arnaud Remay, Sébastien Pineau, and the other members of GenHort INRA Angers and Biogenouest® for genetic experiments. Dr. Thomas Debener (University of Hannover) kindly gave us primer information on rose SSR. Dr. Shogo Matsumoto and the members of the Laboratory of Horticultural Science, Nagoya University helped KK write the MS. The authors gratefully acknowledge Daphne Goodfellow for correcting the English. This work was supported by grants from the *Département de Génétique et d'Amélioration des Plantes*, INRA and *Région Pays de la Loire*.

References

Beavis WD (1998) QTL analyses: power, precision, and accuracy. In: Paterson AH (ed) Molecular dissection of complex traits. CRC Press, New York, pp 145–162

Benlloch R, Berbel A, Serrano-Mislata A, Madueño F (2007) Floral initiation and inflorescence architecture: a comparative view. Ann Bot 100:659–676

Bhatt AM (2005) Inflorescence architecture. In: Turnbull CGN (ed) Plant architecture and its manipulation. Ann Plant Rev, vol. 17. Blackwell Publishing Ltd, New York, pp 149–181

Blackman BK, Strasburg JL, Raduski AR, Michaels SD, Rieseberg LH (2010) The role of recently derived *FT* paralogs in sunflower domestication. Curr Biol 20:629–635

Böhlenius H, Huang T, Charbonne-Campa L, Brunner AM, Jansson S, Strauss SH, Nilsson O (2006) *CO*/*FT* regulatory module controls timing of flowering and seasonal growth cessation in trees. Science 312:1040–1043

Bomblies K, Wang RL, Ambrose BA, Schmidt RJ, Meeley RB, Doebley J (2003) Duplicate *FLORICAULA*/*LEAFY* homologs *zfl1* and *zfl2* control inflorescence architecture and flower patterning in maize. Development 130:2385–2395

Bonnin I, Rousset M, Madur D, Sourdille P, Dupuits C, Brunel D, Goldringer I (2008) *FT* genome A and D polymorphisms are associated with the variation of earliness components in hexaploid wheat. Theor Appl Genet 116:383–394

Bradley D, Ratcliffe O, Vincent C, Carpenter R, Coen E (1997) Inflorescence commitment and architecture in *Arabidopsis*. Science 275:80–83

Brown PJ, Klein PE, Bortiri E, Acharya CB, Rooney WL, Kresovich S (2006) Inheritance of inflorescence architecture in sorghum. Theor Appl Genet 113:931–942

Churchill GA, Doerge RW (1994) Empirical threshold values for quantitative trait mapping. Genetics 138:963–971

Coen ES, Nugent JM (1994) Evolution of flowers and inflorescences. Development Suppl:107–116

Crespel L, Chirollet M, Durel C-E, Zhang D, Meynet J, Gudin S (2002) Mapping of qualitative and quantitative phenotypic traits in *Rosa* using AFLP markers. Theor Appl Genet 105:1207–1214

De Vries DP, Dubois LAM (1984) Inheritance of the recurrent flowering and moss characters in F_1 and F_2 Hybrid Tea × *R. centifolia muscosa* (Aiton) seringe populations. Gartenbauwissenschaft 49:S97–S100

Debener T (1999) Genetic analysis of horticulturally important morphological and physiological characters in diploid roses. Gartenbauwissenschaft 64:S14–S20

Debener Th, Linde M (2009) Exploring complex ornamental genomes: the rose as a model plant. Crit Rev Plant Sci 28:267–280

Debener T, Mattiesch L (1999) Construction of a genetic linkage map for roses using RAPD and AFLP markers. Theor Appl Genet 99:891–899

Dieters MJ, White TL, Littell RC, Hedge GR (1995) Application of approximate variances of variance-components and their ratios in genetic tests. Theor Appl Genet 91:15–24

Dill A, Jung H-S, Sun T-p (2001) The *DELLA* motif is essential for gibberellin-induced degradation of *RGA*. Proc Natl Acad Sci USA 98:14162–14167

Dugo ML, Satovic Z, Millan T, Cubero JI, Rubiales D, Cabrera A, Torres AM (2005) Genetic mapping of QTLs controlling horticultural traits in diploid roses. Theor Appl Genet 111:511–520

Esumi T, Tao R, Yonemori K (2008) Expression analysis of the *LFY* and *TFL1* homologs in floral buds of Japanese pear (*Pyrus pyrifolia* Nakai) and Quince (*Cydonia oblonga* Mill.). J Japan Soc Hortic Sci 77:128–136

Fernandez L, Torregrosa L, Segura V, Bouquet A, Martinez-Zapater JM (2010) Transposon-induced gene activation as a mechanism generating cluster shape somatic variation in grapevine. Plant J 61:545–557

Foucher F, Morin J, Courtiade J, Cadioux S, Ellis N, Banfield MJ, Rameau C (2003) *DETERMINATE* and *LATE FLOWERING* are two *TERMINAL FLOWER1*/*CENTRORADIALIS* homologs that control two distinct phases of flowering initiation and development in pea. Plant Cell 15:2742–2754

Foucher F, Chevalier M, Corre C, SouZet-Freslon V, Legeai F, Hibrand-Saint Oyant L (2008) New resources for studying the rose flowering process. Genome 51:827–837

Grattapaglia D, Sederoff R (1994) Genetic linkage maps of *Eucalyptus grandis* and *Eucalyptus urophylla* using a pseudo-testcross mapping strategy and RAPD markers. Genetics 137:1121–1137

Gudin S (2000) Rose: genetics and breeding. Plant Breed Rev 17:159–189

Hagiwara WE, Uwatoko N, Sasaki A, Matsubara K, Nagano H, Onishi K, Sano Y (2009) Diversification in flowering time due to tandem *FT*-like gene duplication, generating novel Mendelian factors in wild and cultivated rice. Mol Ecol 18:1537–1549

Harberd NP, Belfield E, Yasumura Y (2009) The angiosperm gibberellin-*GID1*-*DELLA* growth regulatory mechanism: how an "Inhibitor of an Inhibitor" enables flexible response to fluctuating environments. Plant Cell 21:1328–1339

Hibrand-Saint Oyant L, Crespel L, Rajapakse S, Zhang L, Foucher F (2008) Genetic linkage maps of rose constructed with new microsatellite markers and locating QTL controlling flowering traits. Tree Genet Genomes 4:11–23

Holland JB, Nyquist WE, Cervantes-Martinez CT (2003) Estimating and interpreting heritability for plant breeding: an update. Plant Breed Rev 22:9–111

Jansen RC, Stam P (1994) High resolution of quantitative traits into multiple loci via interval mapping. Genetics 136:1447–1455

Jung C, Müller AE (2009) Flowering time control and applications in plant breeding. Trends Plant Sci 14:563–573

Kikuchi R, Kawahigashi H, Ando T, Tonooka T, Handa H (2009) Molecular and functional characterization of PEBP genes in barley reveal the diversification of their roles in flowering. Plant Physiol 149:1341–1353

Kitahara K, Matsumoto S (2000) Rose MADS-box genes '*MASAKO C1* and *D1*' homologous to class C floral identity genes. Plant Sci 151:121–134

Kitahara K, Hirai S, Fukui H, Matsumoto S (2001) Rose MADS-box genes '*MASAKO BP* and *B3*' homologous to class B floral identity genes. Plant Sci 161:549–557

Knott SA, Neale DB, Sewell MH, Haley CS (1997) Multiple marker mapping of quantitative trait loci in an outbred pedigree of loblolly pine. Theor Appl Genet 94:810–820

Kobayashi Y, Kaya H, Goto K, Iwabuchi M, Araki T (1999) A pair of related genes with antagonistic roles in mediating flowering signals. Science 286:1960–1962

Kojima S, Takahashi Y, Kobayashi Y, Monna L, Sasaki T, Araki T, Yano M (2002) *Hd3a*, a rice ortholog of the *Arabidopsis FT* gene, promotes transition to flowering downstream of *Hd1* under short-day conditions. Plant Cell Physiol 43:1096–1105

Krieger U, Lippman ZB, Zamir D (2010) The flowering gene *SINGLE FLOWER TRUSS* drives heterosis for yield in tomato. Nat Genet 42:459–465

Krizek BA, Fletcher JC (2005) Molecular mechanisms of flower development: an armchair guide. Nat Rev Genet 6:688–698

Kyozuka J, Konishi S, Nemoto K, Izawa T, Shimamoto K (1998) Down-regulation of *RFL*, the *FLO*/*LFY* homolog of rice, accompanied with panicle branch initiation. Proc Nat Acad Sci USA 95:1979–1982

Lee J, Lee I (2010) Regulation and function of *SOC1*, a flowering pathway integrator. J Exp Bot 61:2247–2254

Linde M, Hattendorf A, Kaufmann H, Debener T (2006) Powdery mildew resistance in roses: QTL mapping in different environments using selective genotyping. Theor Appl Genet 113:1081–1092

Marguerit E, Boury C, Manicki A, Donnart M, Butterlin G, Némorin A, Wiedemann-Merdinoglu S, Merdinoglu D, Ollat N, Decroocq S (2009) Genetic dissection of sex determinism, inflorescence morphology and downy mildew resistance in grapevine. Theor Appl Genet 118:1261–1278

Mimida N, Kotoda N, Ueda T, Igarashi M, Hatsuyama Y, Iwanami H, Moriya S, Abe K (2009) Four *TFL1*/*CEN*-like genes on distinct linkage groups show different expression patterns to regulate vegetative and reproductive development in apple (*Malus* × *domestica* Borkh.). Plant Cell Physiol 50:394–412

Parcy F (2005) Flowering: a time for integration. Inter J Devel Biol 49:585–593

Prusinkiewicz P, Erasmus Y, Lane B, Harder LD, Coen E (2007) Evolution and development of inflorescence architectures. Science 316:1452–1456

Rajapakse S, Byrne DH, Zhang L, Anderson N (2001) Two genetic linkage maps of tetraploid roses. Theor Appl Genet 103:575–583

Remay A, Lalanne D, Thouroude T, Le Couviour F, Hibrand-Saint Oyant L, Foucher F (2009) A survey of flowering genes reveals the role of gibberellins in floral control in rose. Theor Appl Genet 119:767–781

Roberts AV, Blake PS, Lewis R, Taylor JM, Dunstan DI (1999) The effect of gibberellins on flowering in roses. J Plant Growth Regul 18:113–119

Semeniuk P (1971a) Inheritance of recurrent blooming in *R. wichuraiana*. J Hered 62:203–204

Semeniuk P (1971b) Inheritance of recurrent and non-recurrent blooming in 'Goldilocks' × *R. wichuraiana* progeny. J Hered 62:319–320

Shalit A, Rozman A, Goldshmidt A, Alvarez JP, Bowman JL, Eshed Y, Lifschitz E (2009) The flowering hormone florigen functions as a general systemic regulator of growth and termination. Proc Natl Acad Sci USA 106:8392–8397

Silverstone AL, Tseng TS, Swain SM, Dill A, Jeong SY, Olszewski NE, Sun T-P (2007) Functional analysis of *SPINDLY* in gibberellin signaling in *Arabidopsis*. Plant Physiol 143:987–1000

Souer E, van der Krol A, Kloos D, Spelt C, Bliek M, Mol J, Koes R (1998) Genetic control of branching pattern and floral identity during *Petunia* inflorescence development. Development 125:733–742

Spiller M, Berger RG, Debener T (2010a) Genetic dissection of scent metabolic profiles in diploid rose populations. Theor Appl Genet 120:1461–1471

Spiller M, Linde M, Hibrand-Saint Oyant L, Tsai C-J, Byrne DH, Smulders MJM, Foucher F, Debener T (2010b) Towards a unified genetic map for diploid roses. Theor Appl Genet. doi: 10.1007/s00122-010-1463-x

Steber CM, Cooney SE, McCourt P (1998) Isolation of the GA-response mutant sly1 as a suppressor of ABI_{1-1} in *Arabidopsis thaliana*. Genetics 149:509–521

Tian Z, Wang X, Lee R, Li Y, Specht JE, Nelson RL, McClean PE, Qiu L, Ma J (2010) Artificial selection for determinate growth habit in soybean. Proc Natl Acad Sci USA 107:8563–8568

Turck F, Fornara F, Coupland G (2008) Regulation and identity of florigen: *FLOWERING LOCUS T* moves center stage. Annu Rev Plant Biol 59:573–594

Upadyayula N, da Silva HS, Bohn MO, Rocheford TR (2006a) Genetic and QTL analysis of maize tassel and ear inflorescence architecture. Theor Appl Genet 112:592–606

Upadyayula N, Wassom J, Bohn MO, Rocheford TR (2006b) Quantitative trait loci analysis of phenotypic trait and principal components of maize tassel inflorescence architecture. Theor Appl Genet 113:1395–1407

Van Ooijen JW (2004) MAPQTL® 5.0 software for the mapping of quantitative trait loci in experimental populations. Plant Research International, Wageningen

Van Ooijen JW (2006) JoinMap® 4.0 software for the calculation of genetic linkage maps in experimental populations. Plant Research International, Wageningen

Via S (1984) The quantitative genetics of polyphagy in an insect herbivore. II. Genetic correlations in larval performance within and among host plants. Evolution 35:896–905

Voorrips RE (2002) MapChart: software for the graphical presentation of linkage maps and QTLs. J Hered 93:77–78

Wang G, Schmalenbach I, von Korff M, Léon J, Kilian B, Rode J, Pillen K (2010) Association of barley photoperiod and vernalization genes with QTLs for flowering time and agronomic traits in a BC2DH population and a set of wild barley introgression lines. Theor Appl Genet 120:1559–1574

Weberling DF (1992) Morphology of flowers and inflorescences. Cambridge University Press, Cambridge

Xu S (2003) Theoretical basis of the Beavis effect. Genetics 165:2259–2268

Xu Q, Wen X, Deng X (2005) Isolation of *TIR* and non *TIR NBS-LRR* resistance gene analogues and identification of molecular markers linked to a powdery mildew resistance locus in chestnut rose (*Rosa roxburghii* Tratt). Theor Appl Genet 111:819–830

Yan Z, Denneboom C, Hattendorf A, Dolstra O, Debener T, Stam P, Visser PB (2005) Construction of an integrated map of rose with AFLP, SSR, PK, RGA, RFLP, SCAR and morphological markers. Theor Appl Genet 110:766–777

Yan L, Fu D, Li C, Blechl A, Tranquilli G, Bonafede M, Sanchez A, Valarik M, Yasuda S (2006) The wheat and barley vernalization gene *VRN3* is an orthologue of *FT*. Proc Natl Acad Sci USA 103:19581–19586

Yan Z, Visser PB, Hendriks T, Prins TW, Stam P, Dolstra O (2007) QTL analysis of variation for vigour in rose. Euphytica 154:53–62

Zhang LH, Byrne DH, Ballard RE, Rajapakse S (2006) Microsatellite marker development in rose and its application in tetraploid mapping. J Am Soc Hortic Sci 131:380–387